The definitive publisher version is available online at https://doi.org/10.1016/j.gsd.2021.100714

Optimisation of dual coagulation process for the removal of turbidity in source water using streaming potential

H.N.P. Dayarathne [a], Michael J. Angove [b], Shukra Raj Paudel [c,d], Huu Hao Ngo [e], Wenshan Guo [e], Bandita Mainali [a,*]

[a] School of Engineering and Mathematical Sciences, La Trobe University, Bendigo, Australia
[b] Colloid and Environmental Chemistry (CEC) Research Laboratory, Department of Pharmacy and Biomedical Sciences, La Trobe Institute for Molecular Science (LIMS), La Trobe University, Bendigo, Australia
[c] Department of Civil Engineering, Pulchowk Campus, Institute of Engineering, Tribhuvan University, Pulchowk, Lalitpur, Nepal
[d] Department of Environmental Engineering, College of Science and Technology, Korea University, Sejong, Republic of Korea
[e] Faculty of Engineering, University of Technology Sydney (UTS), PO Box 123, Broadway, NSW, 2007, Australia

* Corresponding author.
E-mail address: b.mainali@latrobe.edu.au (B. Mainali).

Keywords:
Dual coagulation
Flocculation
Streaming potential
Turbidity

A B S T R A C T

The charge at the surface of suspended particles and the degree of its neutralisation play an important role for achieving better turbidity removal efficiency in the coagulation process. Therefore, optimisation of the process critically requires continuous measurement or monitoring of surface charge. Streaming potential for this purpose can be considered as a good potential option in dual coagulation system. This study investigated factors that alter the streaming po-tential of source water, including pH, turbidity, humic acid concentration, inorganic coagulants, ionic strength, and polyelectrolyte concentrations. A range of dual coagulation systems were tested using the streaming potential to optimise coagulant doses., And jar test experiments were performed to estimate the extent of floc formation and turbidity reduction. Several inorganic and organic coagulants were combined in dual coagulation systems; Ferric chloride ($FeCl_3$), Titanium chloride ($TiCl_4$), and Aluminium chloride ($AlCl_3$), Non-ionic polyacrylamide (PAM) and anionic polyacrylamide (aPAM). Turbidity removal efficiencies ranged from 83% to 99%. Ti (IV) systems gave the most efficient removal, which was not improved by the addition of polymer. PAM and aPAM added to Al (III) and Fe (III) flocculant systems, did improve the total removal efficiency and the rate of removal, with the effect more pronounced for Fe (III). Overall, PAM yielded the best results, particularly in combination with Fe (III). The streaming potential proved to be an excellent measure of optimum coagulant dosing.

1. Introduction

Drinking water demand around the world has increased enormously alongside rapid population growth. Accessible drinking water sources, including ground and surface waters, are being polluted because of changing climate and other anthropogenic activities (Amiri et al., 2021; Sohrabi et al., 2021). Higher incidences of bushfires and floods are examples of how water supplies are being impacted (Lipczynska-Kochany, 2018; Sjerps et al., 2017). Efficient, effective, simple, and low-cost water treatment methods are required to provide clean and safe drinking water to expanding populations worldwide. Many treatment processes have been widely

investigated over the last few decades, including chemical and physical processes, such as adsorption, coagulation, and membrane filtration (Kaur, 2021; Prajapati et al., 2021; Sadhu et al., 2022). Turbidity is a critical factor in water treatment processes because it significantly impacts water quality (Jeong et al., 2016; Ntambwe Kambuyi et al., 2020; Zheng et al., 2016), as it is a measure of the transparency of water, with turbidity increasing as the concentration of suspended particulates increases. Suspended materials can be diverse and include components such as clays and mineral particles, organic matter, such as humic materials and ash residues from fire, or even microorganisms such as algae and bacteria (Kim and Jang, 2017; Muthuraman and Sasikala, 2014).

Coagulation is a widely used process for the treatment of highly turbid source water and involves the addition of compounds or materials that act by destabilising suspensions, and collecting or gathering dissolved compounds into flocs which then settle out of suspension flocculation and settling (Alvarez-Bastida et al., 2018; Dayarathne et al., 2020; Po Cheng et al., 2006). In most cases, the neutralisation of surface charge controls the efficiency and extent of the coagulation process, so measuring changes in surface charge and ionic composition of the suspension is useful.

Zeta potential, or electrokinetic potential, can be thought of as the electric potential in the interfacial double layer of a charged particle in aqueous suspension, and is a key indicator of the stability of colloidal dispersions. Systems with high zeta potential tend to be electrically stabilised because of electrostatic repulsion between particles of similar charge, while colloids with low zeta potentials tend to coagulate or flocculate. The measurement of the zeta potential is important in water treatment to optimise the dosing of coagulants to modify surface charge and force flocculation. In a water treatment system, it is ideal to have a continuous way of estimating the zeta potential, which could be used to quickly assess changes in surface charge characteristics as coagulants are added. The degree of coagulation of raw water can be monitored through the variation of streaming potential, and as the streaming current increases, it indicates that more coagulant is required to initiate coagulation. The ability to monitor coagulant dosing through a continuous system can significantly reduce the cost of water treatment by better optimisation of coagulant reagent usage.

Dual coagulation is an application of combining two coagulants. In general, metal coagulants are used as the primary coagulant and polyelectrolytes as the secondary coagulant. Metal coagulants can be Al, Fe and Ti salts, or their polymeric forms such as poly ferric chloride/sulphate (PFC/PFS), poly aluminium chloride/sulphate PAC/PAS), poly titanium chloride/sulphate (PTC/PTS). Polymeric metal coagulants can be more efficient than the dissolved metal coagulants because polymerising the metals can increase the positive charge components such as $Al_{13}(OH)_{34}^{5+}$, $Al_{13}O_4(OH)_{24}^{7+}$, $Fe_2(OH)_2^{4+}$, $Ti_2OCl_2(OH)_4$ (Eslami et al., 2019; Sun et al., 2019; Wang et al., 2010; Zhao et al., 2011). Polyelectrolytes can be of positively-, negatively-, or non-charged water-soluble polymers that facilitate adsorption, charge neutralisation, flocculation and strengthening the flocs. Examples include polydimethyldiallylammonium chloride (PD), and polyacrylamide (PAM) (Bolto and Gregory, 2007; Wei et al., 2009). For instance, Wei et al. reported that PFC-PD dual coagulation system helps strengthen flocs and reduced turbidity by 78% (Wei et al., 2010). In some cases, bentonite or kaolinite clay are added to support flocculation (Al-Essa, 2018).

To our knowledge, most of the studies to date have placed their emphasis on the optimisation and monitoring of coagulation process (Saritha et al., 2017; Zainal-Abideen et al., 2012). Few studies have investigated the use of streaming potential for optimising coagulation (Libecki and Dziejowski, 2008), and so this work is intended to fill the gap by assessing the application of streaming potential in dual coagulation process so that real-time monitoring of coagulant dosing requirements (charge neutralisation) can be observed in a water treatment system. This study investigates dual coagulation and optimises coagulant dose with non-charged and negatively charged polyelectrolytes using the streaming potential to guide the dose during the operation of the system. The streaming potential variation was studied with respect to changes in pH, humic acid concentrations, and total turbidity, streaming potential was used to optimise coagulant dose. The coagulation efficiencies of three inorganic coagulants were observed, and floc settling rates of three dual coagulation systems were also compared. Finally, the best coagulant combinations were applied for the removal of turbidity in source water.

2. Materials and methods

2.1. Preparation of coagulants

Inorganic coagulants, $FeCl_3$, $AlCl_3$, $TiCl_4$ (reagent grade), and organic polyelectrolyte, non-ionic polyacrylamide (PAM) (Mw 5.10^3–6.10^3 Da), anionic polyacrylamide (aPAM) (Poly (2-acrylamido-2-methyl-1-propanesulfonic acid) solution average, MW 2×10^3 Da were obtained from Sigma-Aldrich, Australia. $TiCl_4$ coagulant (1%) was prepared in the laboratory by slowly mixing with predetermined Milli Q (MQ) water Mill-Q system (Millipore, Bedford, USA) volume (300 mL) and concentrated $TiCl_4$ solution (>99% purity). Similarly, 3.09 g of $FeCl_3$ (97%) and 3.03 of $AlCl_3$ (99%) were dissolved in 300 mL of MQ water.

2.2. Preparation of test water

Test solutions of varying compositions were prepared to simulate a wide range of source water samples. Humic acid (HA) solutions were prepared from the sodium salt (Sigma Aldrich, Australia), at concentrations 5, 10, 15 mg/L. Solution pH was adjusted using 0.1 M NaOH. Turbidity was adjusted using kaolinite (Sigma Aldrich, Australia), and measured using Turbidity Logger Sensor NLU-231. The sample pH was measured using Laqua Benchtop pH probe, which was first calibrated with standard pH buffers. 5 mg/mL of $CaCO_3$ solution was prepared using $CaCO_3$ (99%) to maintain the $CaCO_3$ at 20 mg/L. Different source water qualities were simulated/synthesised in the laboratory using humic acid sodium salt (HA) solution and kaolinite clay.

2.3. Source water samples

Source water samples were collected from the lake Eppalock area (coordinates: −36.8600511, 144.5047818), which is an important water source for the regional city of Bendigo, Australia. Water samples were collected in sample bottles after rinsing them

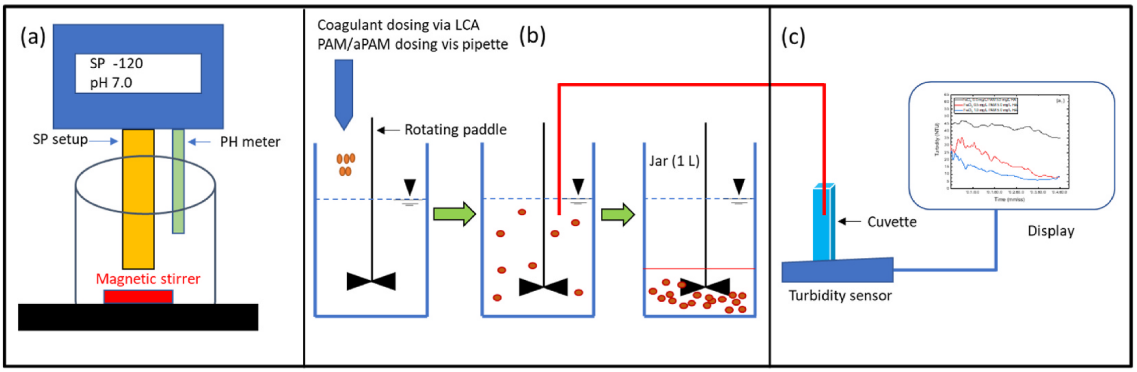

Fig. 1. Schematic diagram of coagulation/flocculation monitoring process: (a) Streaming potential apparatus (LCA), (b) flocculation test/Jar test, (c) measuring turbidity.

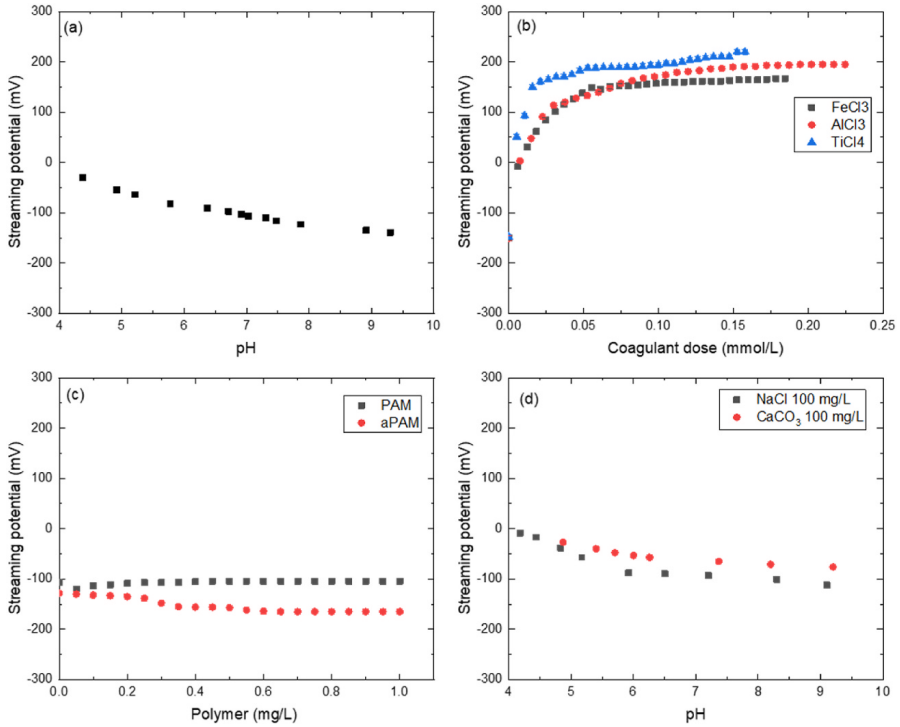

Fig. 2. (a) Streaming potential of MQ water with pH, (b)streaming potential with coagulant dose in MQ water at pH 7 (c) streaming potential with PAM at pH 7 (d) streaming potential with electrolytes at pH 7.

twice with same water, and samples were then taken to the laboratory for further tests and analysis.

2.4. Coagulation and jar tests

Inorganic coagulation tests were performed by adding doses of $FeCl_3$, $AlCl_3$, and $TiCl_4$. For dual coagulant experiments, organic coagulants (0.5 and 1.0 mg/L of PAM/aPAM) were added at the start of rapid mixing.

A lab charge analyser (CHEMTRAC LCA-3) was used to measure the streaming potential of the water samples while adding coagulants and polyelectrolytes (Fig. 1a). The streaming potential is equivalent to the Zeta potential (electrokinetic potential) (Muzi Sibiya, 2014) (Eq. (1)).

$$SP = \Delta P ב D/4\pi\eta k \quad (1)$$

where SP is the streaming potential (unitless), ΔP the press (potential) difference, ב is the electrokinetic potential, D is the relative permittivity of the electrolyte, η is the viscosity coefficient, and *k* is the specific conductivity (Muzi Sibiya, 2014).

The standard jar test (4G Platypus Jar Tester) was carried out to simulate the coagulation and flocculation process. After adding coagulants, water samples were agitated for 3 min at 130 rpm, and then the mixing velocity was reduced to 30 rpm for 7 min to allow for flocculation. Mixing paddles were removed, and a 5-min settling period was allowed (Fig. 1b). Water samples were taken out using a wide-mouthed pipette and placed in a cuvette where the turbidity reduction rate was measured using a turbidity sensor over 5 min

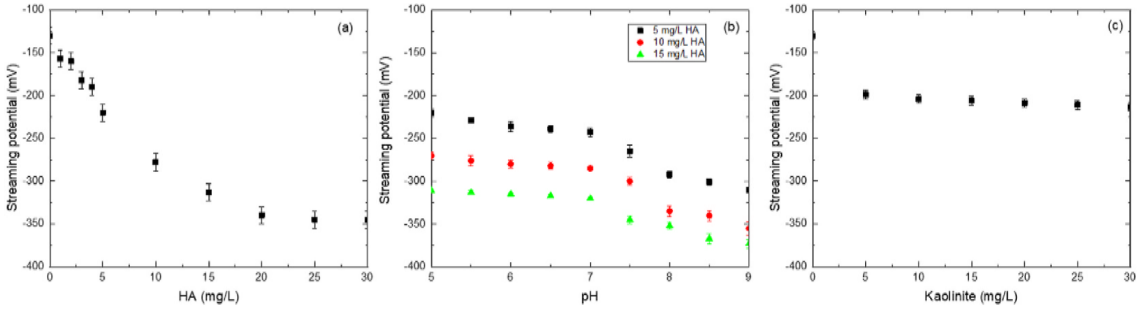

Fig. 3. (a) Streaming potential of MQ water and HA solutions at pH 7, temperature 22 C, (b) influence of pH for streaming potential of HA suspensions (error bars represent SD) (c) streaming potential variation with of kaolinite clay mixed water at pH 7.

(Fig. 1c). The removal efficiency refers to percentage reduction of turbidity which was then estimated by Eq. (2) (Shahid et al., 2019)

$$\text{Removal efficiency } (\%) = (1 - \text{CR/CT}) \times 100 \quad (2)$$

where: C_R and C_T are the turbidity in the raw water and, in the treated water after sedimentation, respectively.

2.5. Statistical analysis

Statistical analysis including standard deviation, mean values were calculated using MS Excel 365 and OrignPro 2019 (Academic) software and all data are presented with standard deviation.

3. Results and discussion

3.1. Measurement of streaming potential

Prior to coagulation experiments, the streaming potential was initially measured at different ranges of turbidity, pH, and HA concentrations to identify how solution conditions affect the value of the streaming potential. In the first set of measurements (Fig. 2a), the pH was adjusted from 4.5 to 9.5 with 0.1 NaOH. Fig. 1a shows that the measured streaming potential varied from −30 to −139 ± 5 mV. The change in the streaming potential with pH is attributed to changing charge on Teflon surfaces (Preočanin et al., 2012).

Fig. 2b demonstrates that the streaming potential increases following the addition of each of the coagulants (2 mg/L of $FeCl_3$, 1 mg/L of AlC_3 and 1 mg/L of $TiCl_4$) at pH 7. The initial streaming potential was close to zero, but increased as the metals formed hydroxide precipitates which carry a positive surface charge at pH 7 (Salg et al., 2013).

Addition of dissolved PAM (Fig. 2c) had little effect on the magnitude of the streaming potential, but addition of aPAM tended to move the streaming potential towards more negative values. This behaviour has been documented in previous studies, and is associated to the result of ionisation of carboxylic acid functional groups that replace some of the amides in aPAM (Qiao et al., 2012).

Fig. 2d presents how the streaming potential measurement was impacted by changing the ionic strength. The addition of salt as NaCl or $CaCO_3$ increased the magnitude of the streaming potential because the electrokinetic potential of the Teflon surface depends on ionic strength (Preočanin et al., 2012). This has also been noted in previous studies (Sun et al., 2016) and likely results from compression of the electric double layer with increasing ionic strength.

The effect of adding aliquots of HA and Kaolinite at pH 7 is presented in Fig. 3. The decrease in streaming potential as HA is added (Fig. 3a) can be attributed to the accumulation of relatively hydrophobic HA molecules at kaolinite surfaces to form a colloidal organic phase. The charge of the HA surfaces will be negative because of ionised carboxylic acid functional groups, and so a negative streaming potential is expected. The kaolinite mineral also possesses a permanent negative charge surface on the siloxane face, and the PZC for the clay is around pH 5, so at pH 7 kaolinite particles also carry a net negative charge which will contribute to an overall negative streaming potential. As the HA concentration is increased, more colloidal material is formed until a maximum streaming potential is reached around −350 mV at 20 mg/L of HA. Further increases in HA probably accumulate at existing colloidal surfaces rather than form new surfaces, so there is no significant increase in total surface charge beyond 20 mg/L of HA. The magnitude of the streaming potential increases with increasing pH (Fig. 3b) because the charge on the HA increases because of increased ionisation of acidic functional groups on HA and the kaolinite surface.

The streaming potential of kaolinite suspensions was measured at pH 7 (without HA). As the amount of kaolinite increased, the streaming potential did not increase significantly; it can be expected that a doubling in the total suspended kaolinite might double the charge which would be reflected in the streaming potential. However, only a small increase from −193 to −219 mV was noted as the solid concentration varied between 5 mg/L and 30 mg/L (Fig. 3c). This is likely because of the flocculation of the suspended kaolinite particles. As mentioned above, at pH 7 kaolinite carries a permanent negative charge on the siloxane faces, but also possesses variable change alumina-like groups on the other clay edges, which will carry a positive charge at pH 7(Van Emmerik et al., 2007). The association of these particles through charge interaction as the kaolinite fraction increases is likely to keep the streaming potential relatively invariant.

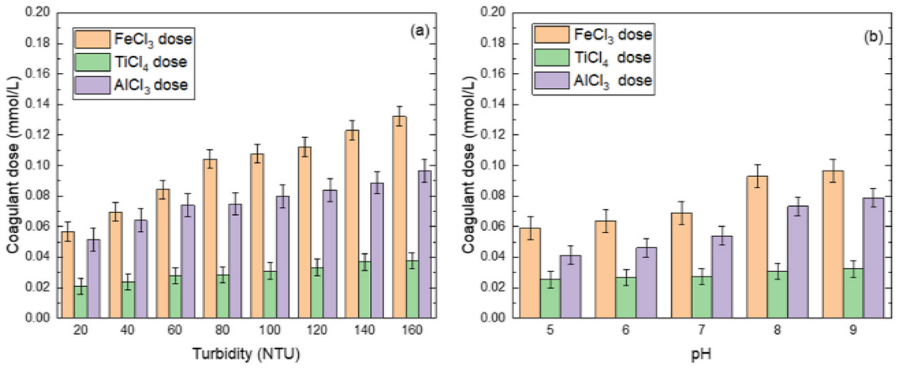

Fig. 4. (a)Turbidity vs. optimum coagulant dose (5 mg/L HA + kaolinite) at pH7 (b) pH vs. optimum coagulant dose of Al, Fe, and Ti coagulants: initial turbidity = 50 NTU. Error bars represent standard errors for 3 replicate experiments.

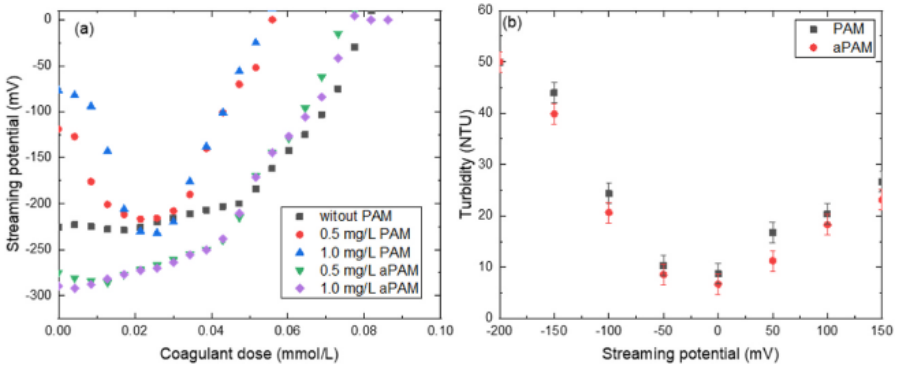

Fig. 5. (a) Streaming potential variation with the addition of coagulant ($FeCl_3$) and with and without PAM or aPAM: 5 mg/L HA and kaolinite at turbidity 50 NTU and pH7. (b) Streaming potential vs residual turbidity. Experiments were performed in triplicate, with points representing mean values, and SD about the size of the data points.

3.2. Synthetic water coagulation

The effect of turbidity on optimum coagulant dose was tested on suspensions of 5 mg/L HA and added kaolinite to adjust the turbidity between 20 and 160 NTU. Fig. 4a shows the coagulant dosages required to reach zero streaming potential at pH 7. Not surprisingly, higher turbidity required higher doses of coagulant. Interestingly though, Fe (III) dose requirements (on a mol/L basis) were higher than for Al (III), whilst Ti (IV) required less than half the Al (III) to reach zero streaming potential.

Although Fe-based coagulants have been favoured in recent times because of their non-toxicity, larger floc size, and superior turbidity reduction, the hydrolysis properties of Fe (III) results in lower polymerisation and inferior coagulation performance compared to Al (III) which quickly produce polymeric species (Chen et al., 2015; Dayarathne et al., 2020). This behaviour typically results in larger dosing of Fe (III) relative to Al (III). The differences between the dosing amount of Fe (III) and Al (III) also indicates that 'sweep coagulation', which results from the interaction of HA molecules with positively charged colloidal hydrolysis products, is the likely mechanism rather than simple charge neutralisation and ionic bridging of the HA by Fe and Al ions. If charge neutralisation were the dominant mechanism, we might expect the Fe (III) to be at least as effective as Al (III).

Lower doses required to achieve coagulation for Ti (IV) compared to Al (III) and Fe (III) is well documented, with the higher charge on Ti making charge neutralisation and bridging adsorption the major mechanisms leading to more efficient coagulation, compared to sweep coagulation for the trivalent ions (Galloux et al., 2015).

The increasing coagulant dose required at higher pH (Fig. 4b) is likely the result of the higher negative-charge and increased solubility of the HA at higher pH values as a greater proportion of the acidic functional groups become ionised, and hence more coagulant is required to collect the increasingly soluble HA at higher pH.

Whilst conventional cationic coagulant systems can be effective, there are several issues around toxicity and expense (Thomas et al., 2020; Zhang and Zhou, 2005). Al and Ti are not desirable inputs because of potential toxicity, and Fe coagulants must be used in higher quantities which can add expense. For these reasons, alternative dual coagulant systems can help reduce the quantity of these materials required and improve the treatment process. This study investigated dual coagulant systems designed with PAM, aPAM and conventional Fe (III) and Al (III) inorganic coagulants. PAM or aPAM was dosed first, followed by Fe or Al. As previously, online streaming current was used to optimise the coagulant dose against the criterion of zero streaming potential.

Fig. 5 (a) shows the streaming potential measurements of a suspension containing 5 mg/L HA and added kaolinite clay to make the total turbidity 50 NTU. The inorganic coagulant was Fe (III), with varying amounts of added PAM or aPAM. Approximately 0.08 mmol/L of Fe (III) was required without added polymer to reach zero streaming potential. When PAM was present at 0.5 mg/L, the required

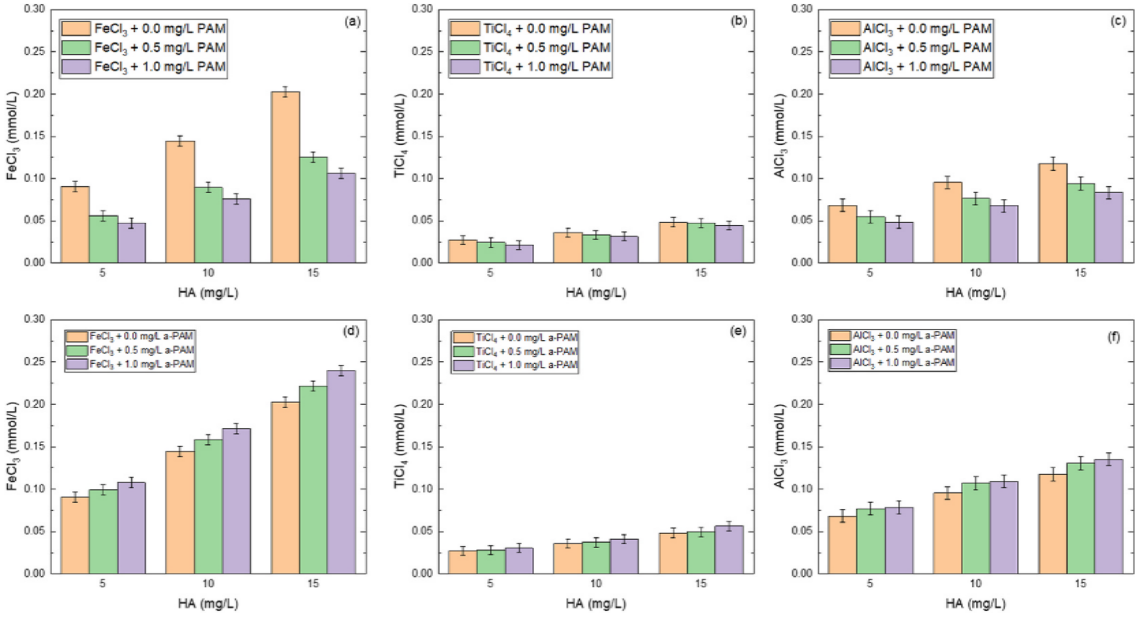

Fig. 6. HA concentration vs coagulant dose at the point of zero stream charge: (a), (b), (c), with PAM, (d), (e), (f) with aPAM, initial pH = 7, HA concertation changed from 5 mg/L to 15 mg/L, PAM concertation changed from 0.0 mg/L, 0.5 mg/L and 1.0 mg/L, Turbidity = 50 ± 2 NTU, Temperature = 22.5 °C (room temperature).

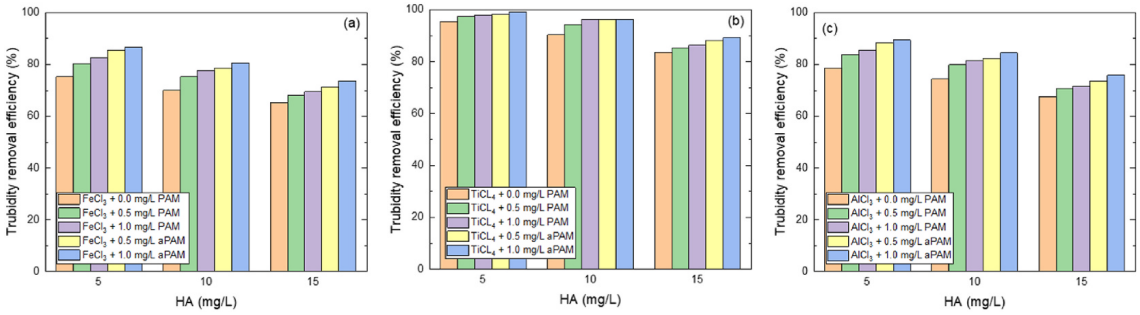

Fig. 7. Turbidity removal efficacy: initial turbidity = 50 NTU, initial pH = 7.

Fe (III) dose was reduced to around 0.05 mmol/L but doubling the PAM to 1.0 mg/L made little difference. An interesting feature of the data in Fig. 4 is that when PAM was present, initial aliquots of Fe (III) reduced the streaming potential to a minimum before it began to increase again at higher Fe (III) additions. The suspensions were also visually different, when PAM was present flocs were larger and more open and gel-like. Without PAM, the flocs were smaller and denser. As Fe (III) was added to the PAM systems, the flocs began to shrink and take on a less voluminous appearance.

The primary role of PAM is to strengthen flocs and promote rapid settling (Huang et al., 2016; Oktaviani and Adachi, 2018), and the PAM clearly makes a visual difference to the floc structure when present. The reduction (tending more negative) in the streaming potential when positively charged Fe (III) is added initially likely results from a rearrangement of floc structure and reflected by the visual change in the floc appearance as the streaming potential falls. Such a rearrangement likely involves the initial chelation of Fe (III) by HA, which then causes a rearrangement at the exterior of the floc structure to expose more negative surface charge to maintain the stability at the water/floc interface. As the Fe (III) concentration increases, more negative charge is neutralised and accompanied by decreased colloidal stability of flocs and a visual change in the floc appearance.

When aPAM was present, higher Fe (III) doses were required to reach zero streaming potential. This is not surprising given that the aPAM carries a negative charge which requires more positively charged Fe (III) to neutralise.

Fig. 5b shows the residual turbidity at various streaming potential values between −200 mV and 150 mV (±5 mV). PAM was added first (1.0 mg/L), and then Fe (III) was added dropwise to adjust the streaming potential. Residual turbidity values were measured after flocculating for 7 min, followed by a 5 min sedimentation time. Using coagulants, streaming potential was set to −150 mV, −100 mV, and −50 mV, zero, 50 mV, 100 mV and 150 mV. The data suggest that residual turbidity reaches a minimum as the streaming potential approaches zero, indicating that zero streaming potential is a good predictor for conditions of optimum flocculation. Systems are less efficiently flocculated at non-zero values of the streaming potential probably because of electrostatic repulsion of the negatively- or positively charged surfaces.

Fig. 6 presents combinations of flocculant doses with and without PAM/aPAM required to achieve zero streaming potential at

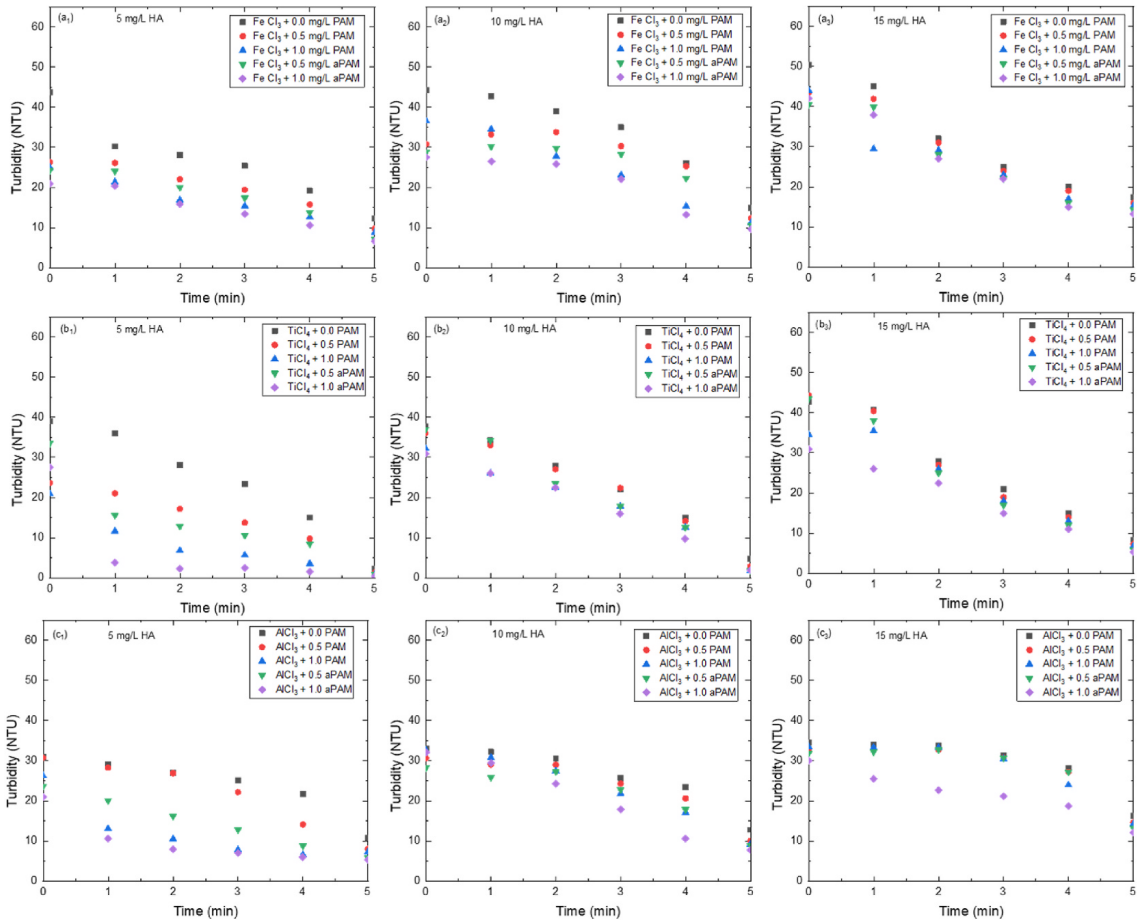

Fig. 8. Effect of dual coagulation on turbidity reduction rate with PAM: (a) $FeCl_3$, (b) $TiCl_4$, (c) $AlCl_3$, initial pH = 7, HA concentration changed from 5 mg/L to 15 mg/L, PAM concentration changed from 0.0 mg/L,0.5 mg/L and 1.0 mg/L, Turbidity = 50 ± 2 NTU, Temperature = 22.5 °C (room temperature).

different HA concentrations. Generally, Ti (IV) dosage was lower than for Fe (III) and Al (III). Adding PAM decreased the amount of Al (III) or Fe (III) required but had no significant effect on the amount of Ti (IV) required.

A similar trend for the aPAM systems was also observed, with lower doses of Ti (IV) required compared to Al (III) and Fe (III). However, again because of the negative charge on the aPAM, higher cation doses were required to reach zero-streaming potential compared to PAM.

An overview of the data in Fig. 6 shows that systems using PAM require lower cation doses than aPAM. Further, the increase in dose of polymer from 0.5 to 1.0 mg/L does not substantially improve the amount of cation required to reach zero streaming potential. However, it must be noted that Fig. 5 only indicates the requirement to reach zero streaming potential, not how efficient the removal of the HA is. To understand the removal aspect total turbidity reduction, and the time it takes to reduce turbidity were measured, with the data presented in Figs. 7 and 8.

Removal efficiencies ranged between 65 and 95% (Fig. 7), with the Ti (IV) systems showed the most significant removal, whilst residual turbidity was higher when the HA concentration was higher. The addition of PAM or aPAM made minor improvements to the removal efficiency and was more noticeable in the Fe (III) and Al (III) systems.

The Floc settling rate was determined by measuring turbidity reduction (NTU) over 5 min with the initial turbidity set as 50 ± 2 NTU. Fig. 8 clearly presents that overall, the Ti (IV) coagulant systems were significantly more efficient at reducing turbidity. The addition of polymer to Ti (IV) did not improve the extent or rate of removal after 5 min, though there is some evidence of faster initial removal when the HA concentration was 5.0 mg/L.

For the Al (III) systems, the addition of polymer dual coagulants improved turbidity reduction when the HA concentration was 5.0 mg/L, but there was little difference between Al (III) and Al (III)+polymer at the two higher HA concentrations.

Addition of PAM or aPAM to Fe (III) systems improved HA removal at all the HA concentrations tested, with the greatest effect at 5.0 and 10 mg/L HA. In fact, the overall results of the settling experiments suggest that it is only in the Fe (III) systems that the addition of polymer makes any substantial improvement to the reduction in turbidity.

3.3. Test results of source water and treatment

The systems studied above were model systems where water composition was controlled. In order to understand how the general findings in these model systems could be more broadly applied, tests were undertaken with water obtained form a natural water system

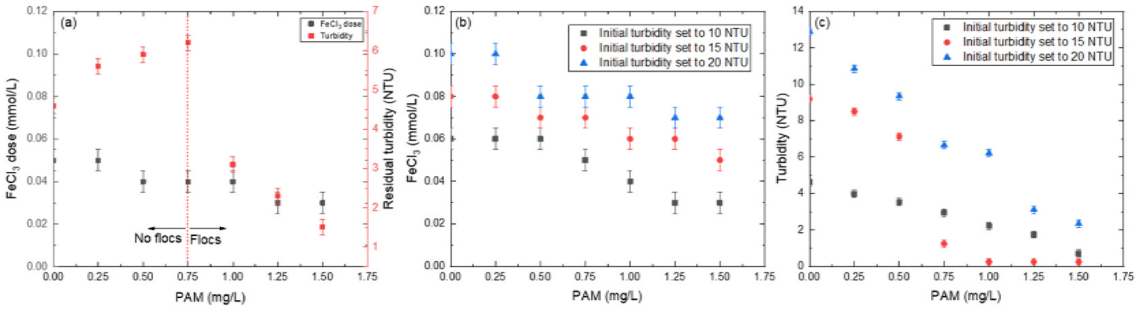

Fig. 9. Optimising $FeCl_3$-PAM dual coagulation for natural waters: (a) residual turbidity value without adding kaolinite, (b) increasing turbidity by adding kaolinite and optimising $FeCl_3$-PAM system, (c) residual turbidity values of $FeCl_3$-PAM system. Temperature maintained at 22.5 °C.

that is used as source water for a larger regional city (Bendigo, Victoria, Australia).

The source water samples are alkaline with a pH around 8 (±1). Based on the electric conductivity of the source water (532 μS/cm), salt enrichment was low (Adimalla and Taloor, 2020). Further, the turbidly of samples water were around 3.4 ± 0.2 NTU, which is above the Australian drinking water standards.

Treatment of this water using a Fe(III)-PAM system resulted in a significant improvement in water quality (Fig. 4), with rapid floc formation and settling at higher turbidity values.

Fig. 9a shows the residual turbidity of treated samples with Fe(III)-PAM, where the amount of Fe (III) added less than for the synthetic water because of the lower initial streaming potential of the natural water. Although flocs were visible with 1.0 mg/L of PAM or more, the residual turbidity was around 4.2 to 6 NTU, and addition of kaolinite was required to bring about efficient settling to remove the turbidity to an acceptable level.

Fig. 9b shows the required addition of Fe (III), and clearly shows that the optimum coagulant dose increases with increasing turbidity, and the Fe (III) amount is reduced as the PAM amount increases. Maximum turbidity reduction was measured to be 0.25 NTU (Fig. 9c) which was the sample having the initial turbidity of 15 NTU.

Current water treatment in the Bendigo region consists of extensive multi-stage treatment using combinations of membrane filtration, UV treatment, and ozonolysis. This is an expensive process with high energy demand. Whilst we are not suggesting that the processes discussed in this study should replace this treatment, the results do show that similar levels of turbidity reduction can be achieved using relatively simple and significantly less expensive treatment options, which might be more viable in communities where access to more advanced water treatment options is problematic.

4. Conclusion

The addition of polymer to ionic coagulation systems can assist in two ways; i) reduce the total amount of ionic coagulant required to achieve flocculation, and ii) increase the rate of settling, thereby increasing the efficiency of turbidity removal. In this study, experimental results suggested that adding PAM polymer to Fe (III) flocculant systems reduced the amount of Fe (III) required to reach zero streaming potential and improved the extent of turbidity removal of waters containing suspended HA and kaolinite. aPAM was not as effective as PAM and increased the dosage of Fe (III). Unlike the Fe (III) systems, the addition of these two polymers to systems containing Al (III) did not make a significant difference in either dosage requirements or recovery efficiency. The Ti (IV) system was the most efficient, requiring the lowest dosage and the best reduction in turbidity, but the addition of polymers did not offer much advantage over just Ti (IV).

Overall, Fe (III) based coagulant systems are favoured because of their lower toxicity, though more limited because Fe coagulants are not as efficient in removing HA and reducing turbidity as other metal cations. This study suggested that in combination with PAM, the Fe (III) dual coagulant system can be made more efficient and offers a cost-effective method of avoiding the use of more toxic Al (III) and Ti (IV) coagulant systems. The process could be applied to a natural source water and achieve a reduction in turbidity similar to that obtained in more complex water treatment process.

Declaration of competing interest

The authors declare that they have no known competing financial interests or personal relationships that could have appeared to influence the work reported in this paper.

Acknowledgments

This research was supported by La Trobe University Post Graduate Research Scholarship (LTUPRS) and La Trobe University Full Fee Research Scholarship (LTUFFRS). The authors thank the editor and anonymous reviewers for their valuable comments and suggestions.

References

Adimalla, N., Taloor, A.K., 2020. Hydrogeochemical investigation of groundwater quality in the hard rock terrain of South India using Geographic Information System (GIS) and groundwater quality index (GWQI) techniques. Groundw. Sustain. Dev. 10, 100288. https://doi.org/10.1016/j.gsd.2019.100288.

Al-Essa, K., 2018. Adsorption of humic acid onto Jordanian Kaolinite clay: effects of humic acid concentration, pH, and temperature. Sci. J. Chem. 6, 1. https://doi.org/10.11648/j.sjc.20180601.11.

Alvarez-Bastida, C., Martínez-Miranda, V., Solache-Ríos, M., Linares-Hernández, I., Teutli-Sequeira, A., Vázquez-Mejía, G., 2018. Drinking water characterization and removal of manganese. Removal of manganese from water. J. Environ. Chem. Eng. 6, 2119–2125. https://doi.org/10.1016/j.jece.2018.03.019.

Amiri, V., Kamrani, S., Ahmad, A., Bhattacharya, P., Mansoori, J., 2021. Groundwater quality evaluation using Shannon information theory and human health risk assessment in Yazd province, central plateau of Iran. Environ. Sci. Pollut. Res. 28, 1108–1130. https://doi.org/10.1007/s11356-020-10362-6.

Bolto, B., Gregory, J., 2007. Organic polyelectrolytes in water treatment. Water Res. 41, 2301–2324. https://doi.org/10.1016/j.watres.2007.03.012.

Chen, W., Zheng, H., Teng, H., Wang, Y., Zhang, Y., Zhao, C., Liao, Y., 2015. Enhanced coagulation-flocculation performance of iron-based coagulants: effects of PO43- and SiO32- modifiers. PLoS One 10, 1–20. https://doi.org/10.1371/journal.pone.0137116.

Dayarathne, H.N.P., Angove, M.J., Aryal, R., Abuel-Naga, H., Mainali, B., 2020. Removal of natural organic matter from source water: review on coagulants, dual coagulation, alternative coagulants, and mechanisms. J. Water Process Eng. 40, 101820. https://doi.org/10.1016/j.jwpe.2020.101820.

Eslami, H., Ehrampoush, M.H., Esmaeili, A., Salmani, M.H., Ebrahimi, A.A., Ghaneian, M.T., Falahzadeh, H., Fard, R.F., 2019. Enhanced coagulation process by Fe-Mn bimetal nano-oxides in combination with inorganic polymer coagulants for improving As(V) removal from contaminated water. J. Clean. Prod. 208, 384–392. https://doi.org/10.1016/J.JCLEPRO.2018.10.142.

Galloux, J., Chekli, L., Phuntsho, S., Tijing, L.D., Jeong, S., Zhao, Y.X., Gao, B.Y., Park, S.H., Shon, H.K., 2015. Coagulation performance and floc characteristics of polytitanium tetrachloride and titanium tetrachloride compared with ferric chloride for coal mining wastewater treatment. Separ. Purif. Technol. 152, 94–100. https://doi.org/10.1016/j.seppur.2015.08.009.

Huang, X., Zhao, Y., Gao, B., Sun, S., Wang, Y., Li, Q., Yue, Q., 2016. Polyacrylamide as coagulant aid with polytitanium sulfate in humic acid-kaolin water treatment: effect of dosage and dose method. J. Taiwan Inst. Chem. Eng. 64, 173–179. https://doi.org/10.1016/j.jtice.2016.04.011.

Jeong, S., Nguyen, T.V., Vigneswaran, S., Kandasamy, J., Dharmabalan, D., 2016. Removal of natural organic matter at the Gunbower water treatment plant in northern Victoria, Australia. Desalin. Water Treat. 57, 9061–9069. https://doi.org/10.1080/19443994.2015.1029006.

Kaur, N., 2021. Different treatment techniques of dairy wastewater. Groundw. Sustain. Dev. 14, 100640. https://doi.org/10.1016/j.gsd.2021.100640.

Kim, K.J., Jang, A., 2017. Evaluation of natural organic matter adsorption on Fe-Al binary oxide: comparison with single metal oxides. Chemosphere 185, 247–257. https://doi.org/10.1016/j.chemosphere.2017.07.007.

Libecki, B., Dziejowski, J., 2008. Optimization of humic acids coagulation with aluminum and Iron(III) salts. Pol. J. Environ. Stud. 17, 397–403.

Lipczynska-Kochany, E., 2018. Effect of climate change on humic substances and associated impacts on the quality of surface water and groundwater: a review. Sci. Total Environ. 640–641, 1548–1565. https://doi.org/10.1016/j.scitotenv.2018.05.376.

Muthuraman, G., Sasikala, S., 2014. Removal of turbidity from drinking water using natural coagulants. J. Ind. Eng. Chem. 20, 1727–1731. https://doi.org/10.1016/j.jiec.2013.08.023.

Muzi Sibiya, S., 2014. Evaluation of the streaming current detector (SCD) for coagulation control. Procedia Eng. 70, 1211–1220. https://doi.org/10.1016/j.proeng.2014.02.134.

Ntambwe Kambuyi, T., Bejjany, B., Lekhlif, B., Mellouk, H., Digua, K., Dani, A., 2020. Design of a continuous-flow single-channel reactor using optimal experimental data from batch reactor for turbidity removal by electrocoagulation. J. Environ. Chem. Eng. 9, 104651. https://doi.org/10.1016/j.jece.2020.104651.

Oktaviani, Adachi, Y., 2018. Effect of mixing intensity on flocculation kinetics of polystyrene latex particles with high-charge density polyelectrolyte at various ionic strengths. Colloid Polym. Sci. 296, 1945–1951. https://doi.org/10.1007/s00396-018-4415-7.

Po Cheng, W., Hwa Chi, F., Fang Yu, R., Shi, P.-Z., 2006. Evaluating the coagulants of polyaluminum silicate chlorides on turbidity removal. Separ. Sci. Technol. 41, 297–308. https://doi.org/10.1080/01496390500460625.

Prajapati, M., Shah, M., Soni, B., Parikh, S., Sircar, A., Balchandani, S., Thakore, S., Tala, M., 2021. Geothermal-solar integrated groundwater desalination system: current status and future perspective. Groundw. Sustain. Dev. 12, 100506. https://doi.org/10.1016/j.gsd.2020.100506.

Preočanin, T., Selmani, A., Lindqvist-Reis, P., Heberling, F., Kallay, N., Lützenkirchen, J., 2012. Surface charge at Teflon/aqueous solution of potassium chloride interfaces. Colloid. Surf. A Physicochem. Eng. Asp. 412, 120–128. https://doi.org/10.1016/j.colsurfa.2012.07.025.

Qiao, Z., Wang, Z., Zhang, C., Yuan, S., Zhu, Y., Wang, J., 2012. PVAm–PIP/PS composite membrane with high performance for CO2/N2 separation. AIChE J. 59, 215–228. https://doi.org/10.1002/aic.

Sadhu, M., Bhattacharya, P., Vithanage, M., Padmaja Sudhakar, P., 2022. Adsorptive removal of fluoride using biochar – a potential application in drinking water treatment. Separ. Purif. Technol. 278, 119106. https://doi.org/10.1016/j.seppur.2021.119106.

Salg, S., Salgı, U., Soyer, N., 2013. Streaming potential measurements of polyethersulfone ultrafiltration membranes to determine salt effects on membrane zeta potential. Int. J. Electrochem. Sci. 8, 4073–4084.

Saritha, V., Srinivas, N., Srikanth Vuppala, N.V., 2017. Analysis and optimization of coagulation and flocculation process. Appl. Water Sci. 7, 451–460. https://doi.org/10.1007/s13201-014-0262-y.

Shahid, M.K., Kim, J.Y., Choi, Y.G., 2019. Synthesis of bone char from cattle bones and its application for fluoride removal from the contaminated water. Groundw. Sustain. Dev. 8, 324–331. https://doi.org/10.1016/j.gsd.2018.12.003.

Sjerps, R.M.A., ter Laak, T.L., Zwolsman, G.J.J.G., 2017. Projected impact of climate change and chemical emissions on the water quality of the European rivers Rhine and Meuse: a drinking water perspective. Sci. Total Environ. 601–602, 1682–1694. https://doi.org/10.1016/j.scitotenv.2017.05.250.

Sohrabi, N., Kalantari, N., Amiri, V., Saha, N., Berndtsson, R., Bhattacharya, P., Ahmad, A., 2021. A probabilistic-deterministic analysis of human health risk related to the exposure to potentially toxic elements in groundwater of Urmia coastal aquifer (NW of Iran) with a special focus on arsenic speciation and temporal variation. Stoch. Environ. Res. Risk Assess. 35, 1509–1528. https://doi.org/10.1007/s00477-020-01934-6.

Sun, C., Qiu, J., Zhang, Z., Marhaba, T.F., Zhang, Y., 2016. Coagulation behavior and floc characteristics of a novel composite poly-ferric aluminum chloride-polydimethyl diallylammonium chloride coagulant with different OH/(Fe3+ + Al3+) molar ratios. Water Sci. Technol. 74, 1636–1643. https://doi.org/10.2166/wst.2016.290.

Sun, H., Jiao, R., Xu, H., An, G., Wang, D., 2019. The influence of particle size and concentration combined with pH on coagulation mechanisms. J. Environ. Sci. 82, 39–46. https://doi.org/10.1016/J.JES.2019.02.021.

Thomas, M., Bąk, J., Królikowska, J., 2020. Efficiency of titanium salts as alternative coagulants in water and wastewater treatment: short review. Desalin. Water Treat. 208, 261–272. https://doi.org/10.5004/dwt.2020.26689.

Van Emmerik, T.J., Sandström, D.E., Antzutkin, O.N., Angove, M.J., Johnson, B.B., 2007. 31P solid-state nuclear magnetic resonance study of the sorption of phosphate onto gibbsite and kaolinite. Langmuir 23, 3205–3213. https://doi.org/10.1021/la062765b.

Wang, T.H., Navarrete-López, A.M., Li, S., Dixon, D.A., Gole, J.L., 2010. Hydrolysis of TiCl4: initial steps in the production of TiO 2. J. Phys. Chem. 114, 7561–7570. https://doi.org/10.1021/jp102020h.

Wei, J., Gao, B., Yue, Q., Wang, Y., Li, W., Zhu, X., 2009. Comparison of coagulation behavior and floc structure characteristic of different polyferric-cationic polymer dual-coagulants in humic acid solution. Water Res. 43, 724–732. https://doi.org/10.1016/J.WATRES.2008.11.004.

Wei, J.C., Gao, B.Y., Yue, Q.Y., Wang, Y., 2010. Strength and regrowth properties of polyferric-polymer dual-coagulant flocs in surface water treatment. J. Hazard Mater. 175, 949–954. https://doi.org/10.1016/J.JHAZMAT.2009.10.101.

Zainal-Abideen, M., Aris, A., Yusof, F., Abdul-Majid, Z., Selamat, A., Omar, S.I., 2012. Optimizing the coagulation process in a drinking water treatment plant – comparison between traditional and statistical experimental design jar tests. Water Sci. Technol. 65, 496–503. https://doi.org/10.2166/wst.2012.561.

Zhang, K., Zhou, Q., 2005. Toxic effects of Al-based coagulants on Brassica chinensis and Raphanus sativus growing in acid and neutral conditions. Environ. Toxicol. 20, 179–187. https://doi.org/10.1002/tox.20093.
Zhao, Y.X., Gao, B.Y., Shon, H.K., Cao, B.C., Kim, J.-H., 2011. Coagulation characteristics of titanium (Ti) salt coagulant compared with aluminum (Al) and iron (Fe) salts. J. Hazard Mater. 185, 1536–1542. https://doi.org/10.1016/J.JHAZMAT.2010.10.084.
Zheng, Q., Yang, X., Deng, W., Le, X.C., Li, X.F., 2016. Characterization of natural organic matter in water for optimizing water treatment and minimizing disinfection by-product formation. J. Environ. Sci. (China) 42, 1–5. https://doi.org/10.1016/j.jes.2016.03.005.